91602
new 82-10

ontario hydro
research division

COMPLIMENTARY COPY

CHARACTERIZATION OF Y-Ba-Cu-O HIGH TEMPERATURE SUPERCONDUCTORS

Report No. 90-67-K

P. Mayer and E. DiBlasio
Advanced Materials Technology
Metallurgical Research Department

ABSTRACT

The objective of this program was to develop capability to characterize structural and microstructural properties of high temperature superconductors (Y-Ba-Cu-O type). The developed techniques and methods can be used to evaluate these materials in components and devices which are of potential benefit to the Corporation. During this program, materials fabrication technology was developed to produce test samples capable of making the high temperature materials with properties exceeding those available commercially. This technology is suitable for transfer to private industry.

job	file	date	report no.
80-566	827.0	August 3, 1990	90-67-K

91602
new 82-10

ontario hydro
research division

CHARACTERIZATION OF Y-Ba-Cu-O HIGH TEMPERATURE SUPERCONDUCTORS

P. Mayer and E. DiBlasio
Advanced Materials Technology
Metallurgical Research Department

EXECUTIVE SUMMARY

The objective of this program, to develop capability to characterize structural and microstructural properties of HTSCs relevant to potential applications at Ontario Hydro, was achieved. Expertise, and investigative techniques and methods were established to assist the Corporation in implementation of superconductor technology into Ontario Hydro's power system.

The developed materials characterization capability is considered to be the minimum necessary needed so that Ontario Hydro can, at present time in combination with other information, reliably evaluate components and devices which are of potential benefit.

The developed techniques and methods were used successfully to characterize HTSC materials made at the Ontario Hydro Research Division and acquired from a commercial supplier. Furthermore, the applicability of these methods to investigate property changes of the HTSCs during storage and use was proven.

The results of all tests which were carried-out as a part of this program indicate that the properties of the HTSC material made at Ontario Hydro Research Division are superior when compared to those supplied by commercial producers. It is suggested that the fabrication technology developed in this program is commercialized and transferred under a license to an Ontario manufacturer.

job	file	date	report no.
80-566	827.0	August 3, 1990	90-67-K

TABLE OF CONTENTS

		Page
1.0	INTRODUCTION	1
2.0	MATERIALS PERFORMANCE PROPERTIES	2
2.1	Functional Properties	3
2.2	Structural Properties	3
2.2.1	Mechanical Strength	3
2.2.2	Temperature Resistance	4
2.2.2.1	Thermal Expansion	4
2.2.2.2	Heat Capacity and Thermal Conductivity	4
2.2.2.3	Thermal Shock Resistance	5
2.2.3	Fatigue Resistance	5
2.2.4	Toughness	5
2.2.5	Wear Resistance	6
2.2.6	Environmental Behaviour	6
2.3	Microstructural Properties	6
2.3.1	Morphology of Grain Structure	6
2.3.2	Porosity/Density	7
2.3.3	Composition	7
3.0	MATERIALS CHARACTERIZATION	8
3.1	Materials Preparation	8
3.2	Sample Preparation	8
3.3	Normal/Superconducting State Transition Temperature Determination	9
3.4	Density Determination	9
3.5	X-ray Diffraction (XRD) Analysis	9
3.6	Grain Structure and Porosity	9
3.7	Energy Dispersive X-ray (EDX) Analysis	10
3.8	Mechanical Properties	10
3.8.1	Test Method	11
3.8.2	Mechanical Properties of "As Made" Materials	12
3.8.2.1	Modulus of Rupture	12
3.8.2.2	Modulus of Elasticity	13
3.8.3	Effect of Thermal Cycling	13
3.8.3.1	Modulus of Rupture	13
3.8.3.2	Modulus of Elasticity	14
3.8.4	Effect of Air Exposure	14
4.0	CONCLUSIONS	14
5.0	RECOMMENDATIONS	15
REFERENCES		16
FIGURES		17
TABLES		32
DISTRIBUTION		Last Page

91-03178/

ontario hydro
research division

To DR. D. MILLS
Director of Research

CHARACTERIZATION OF Y-Ba-Cu-O HIGH TEMPERATURE SUPERCONDUCTORS

1.0 INTRODUCTION

Discovery of superconductivity/1,2/ above the temperature of boiling liquid nitrogen in copper oxide-based systems has led to optimism that superconductors may at last find wide application. While the new class of high-transition-temperature (T_c) superconductors represents a significant technological breakthrough these materials will realize only a small part of their vast potential if a number of significant physical limitations cannot be overcome. These impediments to bulk applications include such structural problems as notch sensitivity, low fracture strength and low toughness. This new class of high-temperature superconductors (HTSCs) is restricted not only by these considerations, but by current-carrying capacities and critical magnetic fields as well. Both structural and functional properties strongly depend on microstructure, which, in turn, is sensitive to manufacturing and processing techniques.

The improvements of HTSC material properties to transform them into engineering materials is a formidable challenge for materials scientists. Successful use of the bulk materials depends on the extent to which the properties can be improved to meet the requirements of specific applications.

Recognizing the potential impact, the discovery of HTSCs may have an Ontario Hydro's power generating, transmission and distribution system, a HTSC Task Force was set-up to address this issue. The purpose of the Corporation-wide working group is to monitor advances in the technology, assess potential applications and spearhead exploitation of short and long term opportunities/3/. An Interim Task Force Report on HTSCs issued in January, 1988, recommended that a 2-year program be undertaken with emphasis on information gathering, application studies and material technology. One of the major tasks in the area of materials technology is to develop the capability to characterize performance properties of HTSCs relevant to potential applications at Ontario Hydro. In the program, carried out by the Metallurgical and Mechanical Research Departments, the issues related to HTSCs performance properties were reviewed and a limited experimental program of material characterization was completed. The experimental program included preparation of materials with controlled composition and density, X-ray powder

diffraction and energy dispersive X-ray analyses, scanning electron microscopy, and studies of thermal cycling and environment effects on mechanical properties.

To date there are four known types of high temperature (T_c) copper oxide superconductors, La_2CuO_4 (T_c = 40K), $YBa_2Cu_3O_7$ (T_c = 93K), Bi-Sr-Ca-Cu-O (T_c = 80 to 110K) and Tl-Bi-Ca-Cu-O (T_c = 80 to 125K). The work in this program was focused on bulk Y-$BA_2Cu_3O_{7-x}$ compound since this material has been studied most extensively and is representative of this class of materials. Other reasons for choosing this material for study are that thallium compounds are highly toxic and bismuth compounds are of marginal interest because they exhibit very low transport current densities.

2.0 MATERIALS PERFORMANCE PROPERTIES

When the HTSC materials are considered for a particular application, three sets of properties must be taken into account: functional, structural and microstructural.

The functional properties of HTSC materials are defined by the relationship between magnetic field (H), temperature (T) and current density (J). This relationship, shown schematically in Figure 1, defines the transition surface from superconductive state to normal state. The critical values of these three variables (J_c, H_c and T_c) can be used to establish design limits for applications of superconductors. These data must be material specific to be useful in engineering design and provide sufficient information needed to assess the suitability of a specific superconductor.

There are six main structural properties commonly used to select engineered materials for structural applications: strength, resistance to extreme temperatures and temperature cycling, fatigue resistance, toughness, wear resistance and environmental behaviour. Frequently, additional criteria must be considered because of other than performance constraints. Typical constraints are existing specifications, availability (the correct size, shape, and quantity), processing equipment limitations (length, width, thickness, or shape), and, of course, cost (material, processing, or shipping).

It is important to keep in mind that the six basic structural properties of materials should be used only as a guide to design a prototype. Functional and performance trials are necessary to optimize the design and refine the materials property requirements to meet the performance and safety criteria.

Since HTSC are ceramic materials, tight microstructural control during manufacture is necessary to achieve and maintain the desired functional and structural properties. The full extent of the microstructural properties effect on the performance of the HTSC is presently not established. However, it is known that the performance properties are affected by the following parameters:

- chemical homogeneity,
- porosity (size, shape, distribution, etc).
- grain size and texture, and
- composition and structure of grain boundaries.

2.1 Functional Properties

A vast body of information exists on measurements of J_c-H_c-T_c relationship for a wide variety of materials since the discovery of HTSC family of materials in 1986. The thrust of the current work is to increase J_c and H_c to meet the requirements of large equipment design (eg, transmission cables $J_c \approx 10^5$ A/cm^2 and $H_c \approx 10$ Tesla, large magnets $J_c \approx 10^5$ A/cm^2 and $H_c \approx 15$ Tesla, etc).

The measurements of J_c, H_c and T_c are performed in the Electrical Research Department and will be reported separately/4/.

The methods to determine these parameters are well established, since they have been used extensively in SC research for many years. There are, however, persistent problems with contacts. A program, supported by the OHRD Director's Fund is in progress to address the contact problems and develop reliable HTSC-metal conductor joints for high current applications.

2.2 Structural Properties

2.2.1 Mechanical Strengths

Ceramics tend to be weak in tension, but strong in compression. Compressive strength is near the tensile strength in metals, but compressive strength may be 10 times the tensile strength in a ceramic. The discrepancy between tensile and compressive strengths is in part due to the brittle nature of ceramics. In tension, ceramics, unlike metals, are unable to yield and relieve the stress. Another important factor is the presence of internal flaws from which cracks can propagate in tension, but not in compression. More important than the number of flaws is flaw size. According to the Griffith relationship for brittle materials, strength is defined as:

$$r = (E2M/\pi C)^{1/2} \qquad (1)$$

where E is the elastic modulus, M is the fracture surface energy, and C is the length of the hole or flaw. Thus, strength decreases as flaw size increases.

Single-phase ceramics usually are stronger than those with more than one phase. When a part cools after sintering, the different phases contract unequal amounts causing residual stresses in the material. Unlike metals, ceramics are unable to relieve such stresses.

Grain size also affects the strength of ceramics. Increasing the average grain size weakens the ceramic. This weakening may occur because larger grain sizes usually bring larger flaws.

Machining can introduce flaws into a part. Sintering to net shape not only saves time and labor, it produces stronger parts. Air can be entrapped during processing. Isostatic pressing under high pressure forces out any trapped air, resulting in a stronger component.

Unlike metals, which are most often tested in tension, ceramics usually are tested in compression or bending. When tensile tests for ceramics are desired, care must be taken to align the grips accurately and apply the load axially to avoid an additional bending or torsional stress, which could significantly decrease the measured strength.

The strength of ceramic materials is statistical in nature. There is a great danger in reporting tables of strength values. Strength is not a material property. What is reported is merely an average, and is highly sensitive to the method of specimen preparation, surface and machining treatments, and test conditions. Test method and specimen size should be reported. For the same test method, large specimens are likely to be weaker than small specimens by virtue of the probabilistic nature of brittle fracture (ie, there is a higher probability of finding a large flaw in a large specimen).

The mechanical properties of the superconducting specimens can be determined using three point bend test which can provide estimates of modules of rupture and modulus of elasticity. The test procedure is described in ASTM C 674-81 standard and was used in this work to establish effect of the environment on the mechanical properties of the HTSCs.

2.2.2 Temperature Resistance

The temperature resistance of ceramics is determined by several properties, including creep resistance, thermal expansion, thermal conductivity, and thermal shock resistance. Only the latter three properties must be considered for HTSCs since the creep is a thermally activated process and does not occur at cryogenic to ambient temperatures.

2.2.2.1 Thermal Expansion

The extent of thermal contraction from room to liquid nitrogen temperature is important because thermally induced stresses are a function of the rate of dimensional changes with temperature. This is an important design parameter affecting the rate with which future devices can be cooled, heated and thermally cycled.

There are basically two methods for determination of linear thermal expansion (contraction), interferometry (ASTM E 289) and dilatometry (ASTM E 228). Both of these are equally useful in measuring properties of HTSCs.

2.2.2.2 Heat Capacity and Thermal Conductivity

These properties must also be considered in design with HTSCs, since both determine the rate of temperature change with time in the material during fabrication and use. Both properties determine thermal stress resistance as well as the operating temperature and temperature gradients. Porosity has profound effect on both parameters.

To measure heat capacity and thermal conductivity, a variety of methods can be used. The most common methods are described in pertinent ASTM Standards (eg, Thermal Conductivity-C 408-82).

2.2.2.3 Thermal Shock Resistance

Basically, this property reflects the ability to withstand thermal stresses generated due to large temperature differences within a single solid body. Such stresses can lead to thermal shock damage, producing fractures that result in catastrophic failure, or causing existing flaws to grow, reducing strength and component integrity.

Resistance to thermal shock can be determined by quenching samples from various known temperatures into a liquid nitrogen bath. The initiation of thermal shock damage can be determined by internal- friction measurements or by visual observation (eg, ASTM C484- 86). Conditions such as shape of sample and cooling mechanism must be controlled carefully since both affect the final results. The shape can change thermal-shock resistance and the medium can influence the rate of surface-heat removal.

The HTSCs fall into the category of elastic materials, which fracture when the surface stress reaches a certain level. Temperature conditions for fracture thus can be easily calculated. However, conditions of surface heat transfer also must be considered in such calculations.

The thermal shock resistance is also dependent on the interaction of the environment with the material during heat cycling. Moisture pick- up is of particular concern in HTSCs, since the carbonates usually form at grain boundaries and thus weaken the cohesive forces between the grains developed during sintering.

2.2.3 Fatigue Resistance

Fatigue is a progressive, localized permanent structural change that occurs in materials subjected to fluctuating stresses. Fatigue may result in crack formation or fracture after a sufficient number of fluctuations (cycles). The material failure results from cyclic stresses which are well below the fracture strength of the material.

It is not altogether clear whether this type of fatigue actually occurs in the HTSCs. However, one category of failure over time under constant load (apperial case of cyclic stressing), known as static fatigue, can potentially occur in the HTSC. Since the HTSCs are susceptible to moisture, static fatigue, or actually stress corrosion cracking promoted by moisture can be anticipated.

2.2.4 Toughness

Toughness is the ability of a material to absorb energy and deform plastically before fracturing; the amount of energy absorbed during both deformation and fracture is a measure of the metal's toughness. The amount of deformation preceding fracture is a measure of ductility, and the force needed to cause fracture is a measure of strength.

If a component must withstand some specified load, strength is the controlling property. Ductility may govern if the material must be formed to a specific shape. Toughness, however, is the limiting property if the component must be able to absorb a certain quantity of mechanical energy without fracturing.

There are two widely reported toughness parameters: notch toughness and fracture toughness, although there are others.

A material's notch toughness is its ability to resist impact when it contains one or more stress raisers (notches) such as design features or fabrication defects. Notch toughness typically is reported as the amount of energy needed to fracture the specimen at a specific temperature.

A metal's fracture toughness (which is related to notch toughness) is its ability to resist the propagation of an existing crack. The value most often reported is the stress intensity required at the crack tip to cause the crack to propagate. It is questionable whether toughness measurements on ceramic samples actually tell much about the material. Toughness data for ceramics often are inconsistent, and strength and toughness do not always respond in the same manner to changes in microstructure or interfacial properties.

The toughness of ceramics often is inconsistent, not so much because the materials are inconsistent, but because of the sensitivity of the measurements to specimen preparation, ie, precracking, getting a crack to grow properly, and specimen alignment. It is anticipated that the HTSCs will behave in the same manner.

2.2.5 Wear Resistance

It is anticipated that the HTSCs will not be used in applications where wear resistance is required.

2.2.6 Environmental Behaviour

The Y-Ba-Cu HTSC material when exposed to ambient air loses gradually the superconductive properties. This is due to moisture pick-up and the formation of barium carbonate on all exposed surfaces, including internal interconnected porosity. Therefore, the material must be protected in a hermetically sealed metallic or organic envelope. Long term stability and durability of this envelope is essential in ensuring proper function of the HTSCs.

2.3 Microstructural Properties

The microstructure of HTSCs is characterized by the morphology of grain structure and spatial distribution of porosity, elements and phases. These factors affect to a significant degree practically all functional and structural properties of the HTSC materials. Therefore, the successful use of these materials depends on the extent to which the microstructure can be controlled to achieve and maintain specified properties. To this end, it is essential that a relationship between the microstructure and materials properties is established and that reliable testing and analytical techniques exist.

2.3.1 Morphology of Grain Structure

The morphology of HTSCs is defined by the size, shape, texture and spatial distribution of grains within the bulk material. The techniques to obtain this information include optical and scanning electron microscopy. Both techniques are established, commonly used and well suited for this purpose. The HTSC

materials can be investigated in a fractured form without any preparation or mounted and metallographically polished. The resolution limits for currently available scanning electron microscopes range from 1.5 to 5 nm (equivalent magnification 40,000 x to 130,000 x. The best optical microscopes have resolution limits from 100 to 200 nm (equivalent magnification 1000 x to 2000 x).

The morphological information which can be obtained through the use of scanning electron microscopy is sufficiently detailed to characterize the HTSC material's grain structure, ie, size, shape and spatial distribution.

2.3.2 Porosity/Density

One of the most serious impediments to increasing the performance properties of the bulk HTSCs is porosity. The flux pinning at pores and grain boundaries limits the achievement of current densities of the order of 10^4 to 10^6 A/cm^2 (values of up to 1000 A/cm^2 are usually reported). Reductions in porosity can be achieved by decreasing the starting particle size and the use of higher temperatures and longer sintering times. However, some porosity will always remain because the pores shrink at a rate lower than the sintering process at grain boundaries.

The techniques to obtain information on the amount, size and spatial distribution of porosity are the same as for the morphology investigations.

Additional information on the bulk porosity of sintered HTSC materials can be obtained by measuring apparent density according to ASTM Standard C373-72 or by determining this quantity from physical size and weight.

2.3.3 Composition

All performance properties of HTSCs are dependent on chemical homogeneity (phase and elemental) of the bulk material and grain boundaries. Chemical homogeneity is the basic indicator of the material quality, since the best material is composed of one phase compound $YBa_2Cu_3O_{7-x}$, with no detectable residuals of starting or other materials in the Y_2O_3-BaO-CuO_x system. In addition, it isimportant that the material is homogeneous on microscopic scale and that grain boundaries are free of contamination and corrosion products.

The phase composition and homogeneity can be checked by two methods. The x-ray powder diffraction (XRPD) is suitable for bulk analysis. This method is fast and requires less than one hour for major phase identification and up to 16 hours for trace phase confirmation. Second method, transmission electron microscopy (TEM), should be used when it necessary to confirm the phase homogeneity on a microscopic scale and to investigate grain boundary composition, grain substructure, etc. The TEM method, however, requires a great deal of time to prepare the samples and interpret the results. But, when combined with EDX analysis, can yield valuable information about microstructural features not obtainable any other way.

The elemental composition and homogeneity can be best determined by one of the analytical techniques based on electron optics, such as electron microscopy coupled with x-ray spectrometry, Auger microprobe analysis, etc. A scanning electron microscope equipped with energy dispersive x-ray spectrometer (EDX) can be used to check the elemental composition and spacial distribution very accurately and reliably. Modern instruments use sophisticated data reduction programs for ZAF corrections (Z-atomic number, A-absorption, and F-fluorescence).

3.0 MATERIALS CHARACTERIZATION

The purpose of the experimental program was to develop a capability to determine performance properties of HTSCs using existing materials characterization techniques. These included:

- determination of critical transition temperature (Tc) from normal to superconducting state,
- density measurements,
- X-ray powder diffraction (XRD),
- scanning electron microscopy (SEM),
- energy dispersive X-ray spectrometry (EDX),
- effect of thermal cycling on mechanical strength, and
- effect of environment on mechanical strength.

In order to carry out this work HTSC material samples with variable density and composition were used. Since these were not available commercially or from other OHRD Departments, it was necessary to produce them in our laboratory.

3.1 Materials Preparation

The HTSC material Y $Ba_2Cu_3O_{7-x}$ and its composition variations (see Table I) were prepared from mixture of Y_2O_3 (yttrium oxide), $BaCO_3$ (barium carbonate) and CuO (copper oxide) by solid state reaction (calcining) at elevated temperature. The ingredient powders were dry mixed in a ball mill containing 0.5 inch diameter high density alumina balls. The batches were formulated to yield 400 g ofmixture. The mixing was followed by calcining at 905°C for 18 hours to form the HTSC compound. After completion of the calcining step, the compound was cooled down to 545°C and heat treated in flowing oxygen for 6 hours. The resulting powder was crushed and ground by hand and treated at the above conditions two more times.

3.2 Sample Preparation

The $YBa_2Cu_3O_{7-x}$ compound and its variations prepared by calcining and heat treating in flowing oxygen were dry ground and pressed into rectangular bars (L = 25.4 mm, W = 6.4 mm, T = 3.2 mm). The platelets were produced in a hardened steel die using 207 MPa (30,000 lb/in^2) pressing pressure. No organic binder was used to minimize the contamination of the compound. The pressing was followed by sintering at three different temperatures 945, 965 and 985°C for 18 and 67 hours to produce samples with different density. The mixtures other than $YBa_2Cu_3O_{7-x}$ were sintered at 945°C. The heat up and cool down rate was 5°C/minute. Heat treatment in flowing oxygen was done at 545°C for 6 hours.

3.3 Normal/Superconducting State Transition Temperature

Conventional four-terminal technique was used to characterize the normal to superconducting state transition of $YBa_2Cu_3O_{7-x}$ material made in our laboratory. Figure 2 shows a typical result of these measurements. The sample exhibits a semiconducting behaviour until transition to superconductive state at about 96°C.

3.4 Density Measurements

The apparent density of the HTSCs produced in our laboratory was determined from physical size and weight of sintered samples.

Using this method, the effect of sintering temperature and time on density of $YBa_2Cu_3O_{7-x}$ material was investigated. The data given in Table II and Figure 3 illustrate the effect of these variables on the material densification. These results were obtained during density optimization experiments starting with a 18 hours sintering cycle at 945°C. The 67 hour sintering cycle at 985°C produces material with density about 85% theoretical. This density is comparable to that reported in the literature/5/ achieved by a partial melting procedure, consisting of ten seconds exposure of the material to 1200°C.

3.5 X-Ray Diffraction (XRD) Analysis

The X-ray diffraction analysis of sintered $YBa_2Cu_3O_{7-x}$ material indicated that the samples consist of the superconducting orthorhombic phase with no secondary phase detected. A typical detection limit of secondary phase for this type of material is about 0.5%.

3.6 Grain Structure and Density

Scanning electron microscopy was used to investigate the grain structure morphology of selected samples in order to reveal their internal structure. The observations were performed on metallographically polished cross-sections and mechanically fractured surfaces.

Figures 4 to 7 show structural features of metallographically polished cross-sections through samples No. 1, 4, 7 and 12. These cross-sections are typical and illustrate very well the real features of the structure, and the preparation and polishing artifacts.

Figure 4 shows that the single phase $YBa_2Cu_3O_{7-x}$ compound structure is composed of elongated grains up to 100 μm in length and up to 15 μm in width. The sample also indicates the presence of significant amount of voids. Some of these are polishing artifacts, others are real residual porosity left in the sample after sintering. It is a difficult task to establish which of the voids visible on the micrograph are real residual porosity. Usually, the shape of real residual pores is more rounded and regular than the voids caused by material removal during polishing. The pores of a well sintered sample are found at two locations: at triple points where three grain boundaries meet and in the middle of grains.

Only rarely, residual pores can be found at a boundary between two grains. The ability to distinguish real features and artifacts improves substantially with experience of the observer and care given to the sample preparation.

Electron microscopy, when used in the backscattered electron detection mode can be used to distinguish phases with a different crystallography or elemental composition. Figures 5 to 7 illustrate this capability of the SEM technique. Further analysis using EDX technique provide elemental composition of these phases, without removal from the analytical instrument. If necessary, XRD analysis can be performed to determine crystallographic structure of these phases.

Additional information on the amount, size and spatial distribution of porosity can be obtained by investigating fractured samples in the SEM. Figures 8 to 12 illustrate the type of porosity typically found in $YBa_2Cu_3O_{7-x}$ materials. In Figure 8, two types of pores can be readily seen: trapped voids inside of the grains indicating growth, and residual packing porosity at grain boundaries. Using computerized image analysis, various aspects of the porosity including density can be established and statistically treated.

3.7 Energy Dispersive X-Ray (EDX) Analysis

Table III illustrates a typical example of $YBa_2Cu_3O_{7-x}$ material elemental analysis. Composition of a homogeneous, one phase material can be routinely determined to better than ±0.1 at %. This method of analysis can be used reliably as quality control or acceptance test when required.

This method of elemental analysis not suitable for multi-phase and non-homogeneous samples. Table IV contains the analysis results of three (No 4 and 7) and two (No 12) phase samples. The analyzed compositions are significantly different from the nominal compositions. For this type of sample other analytical methods must be used which are not sensitive to the microscopic non-homogeneity of the multiphase structures.

3.8 Mechanical Strength

Thermal cycling from room to boiling liquid nitrogen temperature and exposure to ambient environment can have a profound effect on the integrity of the HTSCs. Loss of mechanical strength is usually the best indication of the extent of the integrity deterioration. Thus, in this program a simple three point bend test

technique was chosen to provide estimates of two basic parameters which characterize the mechanical properties. These are: modulus of rupture* and modulus of elasticity**.

3.8.1 Test Method

The test procedure used in this work is based on ASTM C674-81; a test method for determination of the modulus of rupture and the modulus of elasticity of brittle ceramic bodies. In this test, the specimens are supported on two small diameter pins and a direct load is applied at the midpoint between the supports at a uniform rate until breakage occurs.

The test system (MTS #810 Material Tests System, MTS #442 Controller, MTS #410 Function Generation, MTS #20488220KiP Actuator, Houston Omnigraph 2000 Recorder and Strainsert 250 lb capacity load cell S/N 09231-1) was equipped with a loading assembly schematically shown in Figure 13. This assembly was fabricated specifically to suit the dimensions of samples utilized in this study. Furthermore, the assembly was designed to ensure proper alignment of the load bearing pins for uniform application of force. The specimen support and loading pins were made from Ni-Cr Alloy 8620 (case hardened to depth of 0.8 mm, R_c = 60 - 62 at surface).

Rectangular specimens (nominal dimensions L = 25.4 mm, W = 12.7 mm and T = 6.4 mm) were tested without any surface preparation in as made condition or after exposure to a specific environment. All due precautions were observed not to damage the surface in any way since the properties of this type of material are very sensitive to surface defects. The specimens were stored in an electric oven at 70°C after fabrication and environmental testing. Before mechanical testing the samples were allowed to cool to room temperature in a desiccator.

During the mechanical test, the specimens are placed on the support pins, spaced 19.1 mm between centres, with the specimen overhanging at each end by the same length. The loading pin was positioned midway between the supporting pins. The load was applied at a right angle by the plunger through this pin at a rate of 4 mm/min until failure. During this time load and the plunger travel (deflection) were recorded. These recordings were linear except for cases where there was an early failure of the sample due to a large defect.

---

* Breaking strength of a non-ductile solid as measured by bending.

** A measure of the stiffness of material. Ratio of stress, within proportional limit, to corresponding strain.

The modulus of rupture was calculated from the measured data as follows:

$$M = 3\,PL/2bd^2$$

where:
- E = modulus of elasticity (MPa),
- M = modulus of rupture (MPa),
- P = load at rupture (N),
- L = distance between supports (mm),
- b = width of specimen (mm), and
- d = thickness of specimen (mm).

The recordings of load-deflection were used to generate the load and specimen deflection data needed to calculate modulae of elasticity. These data were determined the mid point between zero load and elastic limit of the sample (elastic range represented by a straight line). The modulae of elasticity were then calculated at this point as follows:

$$E = WL^3/4\delta bd^3$$

where:
- E = modulus of elasticity (MPa),
- W = load coordinate of the selected point (N),
- L = length of span (mm),
- δ = deformation coordinate of the selected point (mm),
- b = width of specimen at the center (mm), and
- d = thickness of specimen at the center (mm).

The results of tests and calculations are summarized in Tables V and VI and illustrated in Figures 15 to 18.

3.8.2 Mechanical Properties of "As Made" Material

The results of mechanical properties tests performed on as made material are given in Tables V and VI.

3.8.2.1 Modulus of Rupture

The values of modulus of rupture for the OHRD made material were found to vary between 35 and 65 MPa, with the largest number of values between 50 and 60 MPa. The average calculated from all measurements is 53.68 MPa. There is a large scatter of the data which is probably caused by the unpredictable nature and extent of the defects in the samples, other than porosity. Generally, the values of the modulus of rupture increase with smaller and fewer defects. Density has a similar effect. Reduction in porosity leads to higher values of fracture modulus, which is consistent with the fact that porosities tend to behave as stress concentrators. The trend observable in Figure 15 appears to confirm this relationship between porosity and mechanical strength.

The values of modulus of rupture for comparable commercially made material were found to be significantly lower than those for OHRD made material. The measured values of 16.57 and 21.95 MPa are on the average three times lower.

The OHRD made material is stronger than materials made using special techniques /5/ to enhance their mechanical properties. The reported values in the literature for these materials are: hot pressed (31 MPa), Cu-composite containing 15% Cu (37 MPa), polymer composite (44 MPa) and partially melted (35 MPa).

3.8.2.2 Modulus of Elasticity

The values of modulus of elasticity for the OHRD made material were found to vary between 10.5 and 54.7 GPa, with the largest number of values between 10 and 25 GPa. The calculated average from all measurements is 19.58 GPa. As for the modulus of rupture the scatter of the data is significant and caused possibly by the unpredictable nature and extent of the defects in the samples. The plot of modulus of elasticity versus sample density (Figure 16) does not indicate any dependence for the OHRD made materials.

The values of modulus of elasticity for comparable commercially made material were found to be lower than those for the OHRD made material. The measured values of 6.83 and 7.51 GPa are on the average two times lower.

The elasticity of the OHRD made material is comparable with materials made using special techniques /5/ to enhance their mechanical properties. The values reported in the literature for these materials are: hot pressed (13 GPa), Cu-composite containing 15% Cu (18 GPa), polymer composite (28 GPa) and partially melted (14 GPa).

3.8.3 Effect of Thermal Cycling

The thermal cycling tests of the OHRD made materials were performed in laboratory atmosphere and consisted of immersion in boiling liquid nitrogen bath (LN_2) for 5 minutes and a 5 minute warm-up in a drying oven set at 50°C. The samples were tested using the three point bend test method (described in Section 3.8.1) after 2, 10, 20 and 100 cycles. The results are given in Table V.

The surface of the samples during the thermal cycling become covered with a white powdery substance, $BaCO_3$. This compound was formed by interaction of the $YBa_2Cu_3O_{7-x}$ compound and atmospheric CO_2 when the surface was covered with frost or water after withdrawal from the liquid nitrogen bath.

Scanning electron microscopy showed that the barium carbonate also forms inside the body of the sample in the interconnected channels of porosity. Figure 17 illustrates how surfaces of these channels become increasingly covered with particles of $BaCO_3$. It is believed that a similar process could have occurred at the boundaries between the grains.

3.8.3.1 Modulus of Rupture

The results of the modulus of rupture measurements on the OHRD made material are plotted as a function of number of thermal cycles in Figure 18. The values show

significant scatter, but a trend can be established by connecting the maximum and average values for each tested number of cycles by lines. Both curves exhibit a sharp drop (-50%) in the modulus of rupture with a minimum at 20 thermal cycles. There is a slight increase in the modulus of rupture at 100 thermal cycles.

3.8.3.2 Modulus of Elasticity

The results of the modulus of elasticity measurements on the OHRD made materials are plotted as a function of number of thermal cycles in Figure 19. The values show again a significant scatter, but a trend can be established by connecting the maximum and average values for each tested number of cycles by lines. Both curves exhibit a sharp drop after few cycles with no further change after 10 cycles.

3.8.4 Effect of Air Exposure

The exposure to laboratory air (30-35% R.H. at -22°C) for up to 80 days has no measurable effect on both mechanical properties (modulus of rupture and elasticity). The measured values are listed in Table VI and plotted as a function of exposure time in Figures 20 and 21. Although the lines drawn through the maximum and average values of the measurements after each period of exposure show variability, no significant dependence can be established. The scatter of the measured values is too large.

4.0 CONCLUSIONS

The major focus of this program was to develop a capability to characterize structural and microstructural properties of HTSC materials relevant to potential applications at Ontario Hydro. This goal was achieved. As a result expertise and characterization techniques and methods were established to assist the Corporation's efforts to implement the superconductor technology into the power system.

The capability, developed in this program, is considered to be the minimum necessary required to meet the Corporation's needs at the present time. The accumulated expertise and the ability to characterize materials can provide a sufficient information base so that Ontario Hydro can reliably identify/design, specify, acquire/build, and evaluate components and devices which are of potential benefit. In particular, the following characterization techniques and methods were developed/applied and evaluated for HTSCs:

- density determination,
- crystallographic structural analysis,
- bulk and micro compositional analysis,
- morphology of grain structure determination,
- porosity size and distribution determination,
- modulus of rupture determination, and
- modulus of elasticity determination.

These techniques and methods were successfully applied to characterize HTSC materials made at the Ontario Hydro Research Division and acquired from a commercial supplier. Furthermore, the applicability of these methods to

investigate the changes of properties of HTSCs during storage and use was proven.

The results of all tests which were performed in this program indicate that the properties of the HTSC material made at the Ontario Hydro Research Division are superior to those supplied by commercial producers. The density, homogeneity (crystallographic and elemental), strength and elasticity are all significantly higher than commercially available materials. Furthermore, the OHRD material was made at much lower cost than quoted by suppliers from USA and Germany. This production technology, yielding superior quality product at comparatively low cost, may be of interest to commercial manufacturers.

5.0 RECOMMENDATIONS

The development of power system devices and equipment incorporating high temperature superconducting materials is progressing rapidly. Ontario Hydro is well positioned to take advantage of this advancing technology due to expertise and capabilities developed in the Corporation-wide HTSC material program.

It is recommended to maintain the capability to characterize HTSCs at Ontario Hydro Research Division to support existing and future developmental, evaluation and testing projects. Currently the capability is used to support one of the Director's Fund projects on the development of contacts for high current applications. It is anticipated that several projects on development and testing of small devices based on HTSC materials will be initiated in the near future.

The technology of making high performance $YBa_2Cu_3O_{7-x}$ material of consistent quality, developed in this project should be commercialized. It is suggested that the technology is transferred under a license to an Ontario manufacturer. This arrangement would provide Ontario Hydro with a source of material of suitable quality if needed and opportunity to recover the developmental costs.

Approved by:

J. Brown
Manager
Metallurgical Research Dept

Submitted:

P. Mayer
Program Manager
Advanced Materials Technology
Metallurgical Research Department

E. DiBlasio
Technologist
Advanced Materials Technology
Mechanical Research Department

PM:cs

REFERENCES

1. J.G. Bednorz and K.A. Muller, Z. Phys. B. 64, 189 (1986).

2. M.K. Wu et al., Phys. Rev. Lett., 58, (1987).

3. HTSC Task Force, "Interim Task Force Report on High Temperature Superconductivity", OHRD Report 87-314-K, January 1988.

4. A.V. Manolescu, P. Mayer, F.Y. Chu and S.G. Krishnasamy, "Development of High Temperature Superconductor - Metallic Conductor Contacts for High Current Applications", OHRD Report, In preparation.

5. K. Salama et al., Journal of Metals, August 1988.

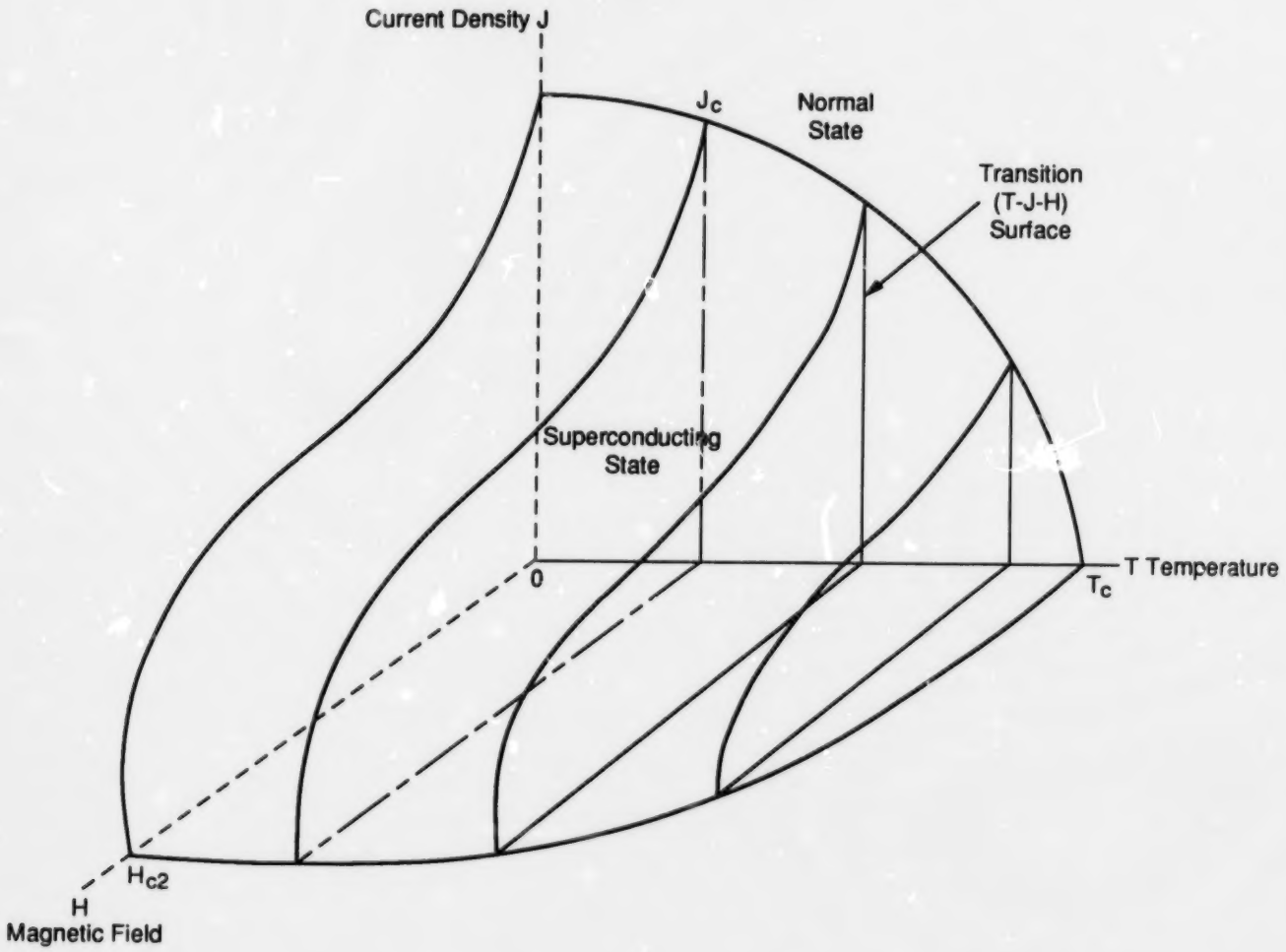

FIGURE 1

TRANSITION SURFACE FROM THE SUPERCONDUCTING TO THE NORMAL STATE.

182362-A23-RD

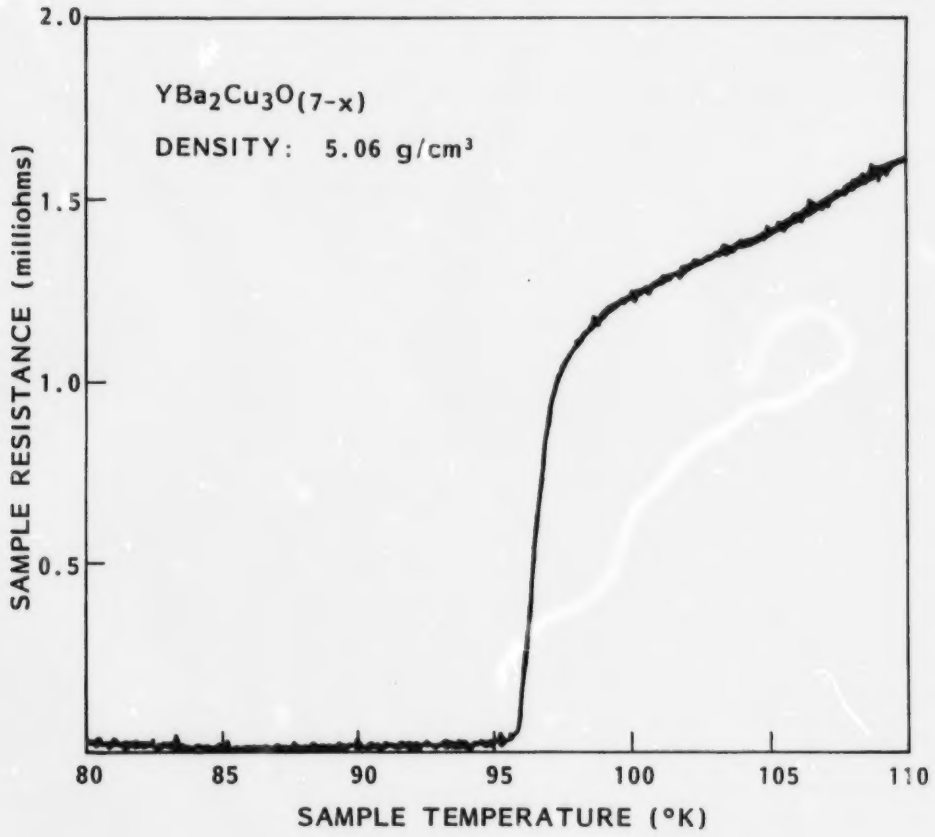

FIGURE 2

RESISTANCE OF $YBa_2Cu_3O_{(7-x)}$ MATERIAL AS A FUNCTION OF TEMPERATURE INDICATING TRANSITION FROM SUPERCONDUCTING TO NORMAL STATE.

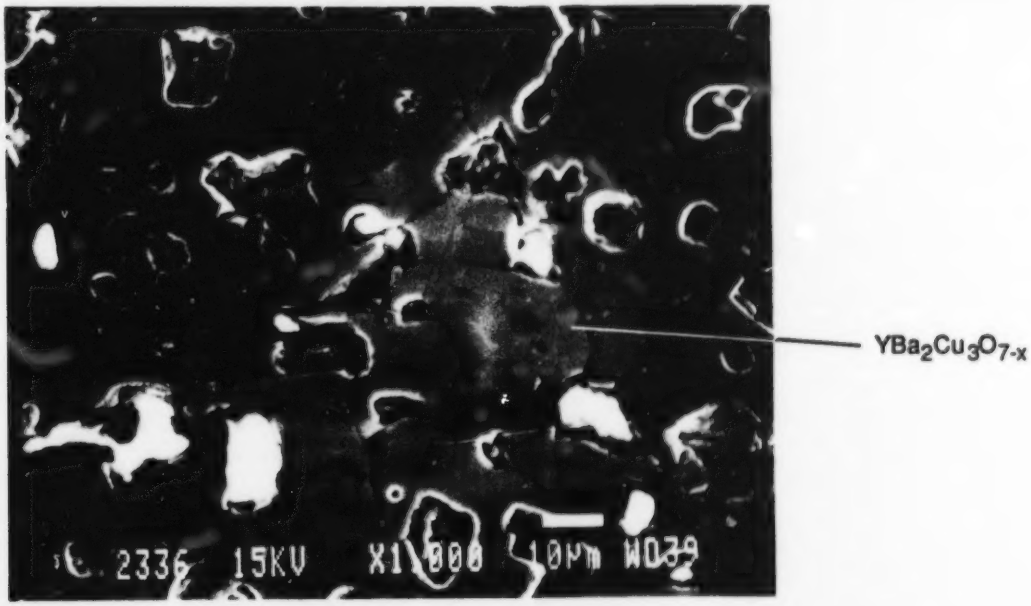

FIGURE 4

SCANNING ELECTRON MICROGRAPH OF SINTERED AND MECHANICALLY POLISHED $YBa_2Cu_3O_{7-x}$ COMPOUND [SAMPLE NO 1 (1 - 2 - 3)] ONE PHASE .

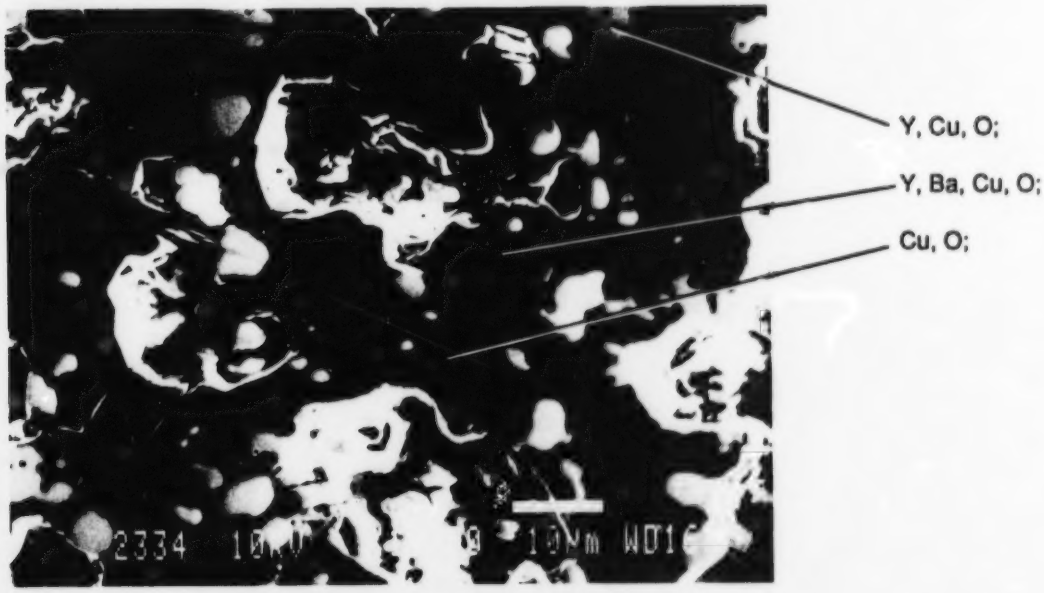

FIGURE 5

SCANNING ELECTRON MICROGRAPH OF SINTERED AND MECHANICALLY POLISHED Y-Ba-Cu-O MIXTURE [SAMPLE NO 4 (1.5 - 2 - 3)]. THREE PHASES CONTAINING DIFFERENT ELEMENTS ARE SHOWN.

182354-K8-RD

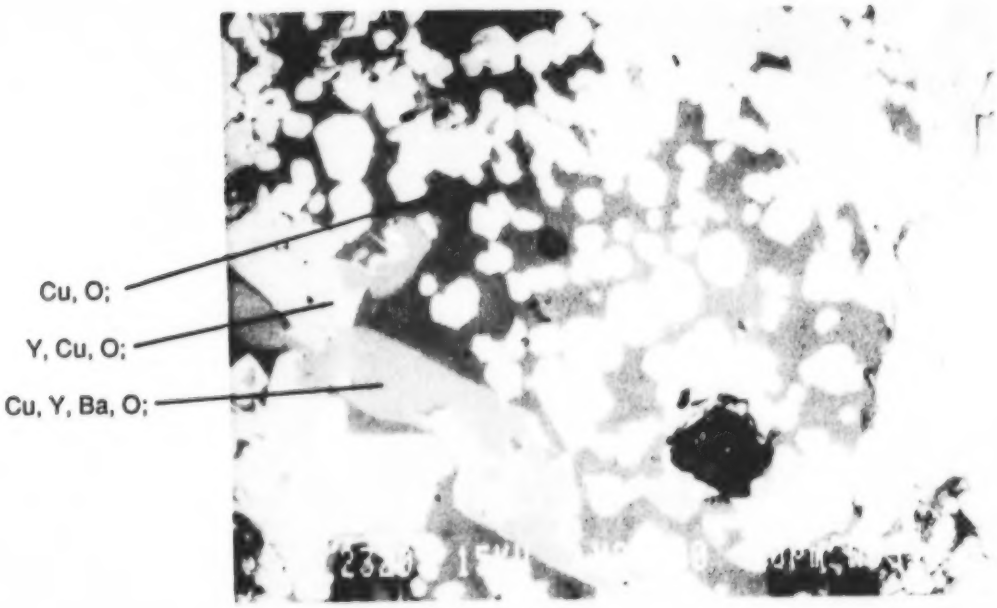

FIGURE 6

SCANNING ELECTRON MICROGRAPH OF SINTERED AND MECHANICALLY POLISHED
Y-Ba-Cu-O MIXTURE [SAMPLE NO 7 (1-1-3)].
THREE PHASES CONTAINING DIFFERENT ELEMENTS ARE SHOWN.

FIGURE 7

SCANNING ELECTRON MICROGRAPH OF SINTERED AND MECHANICALLY POLISHED
Y-Ba- Cu-O MIXTURE [SAMPLE NO 12 (1-2 --3.5)].
TWO PHASES CONTAINING DIFFERENT ELEMENTS ARE AS SHOWN.

182355-K8-RD

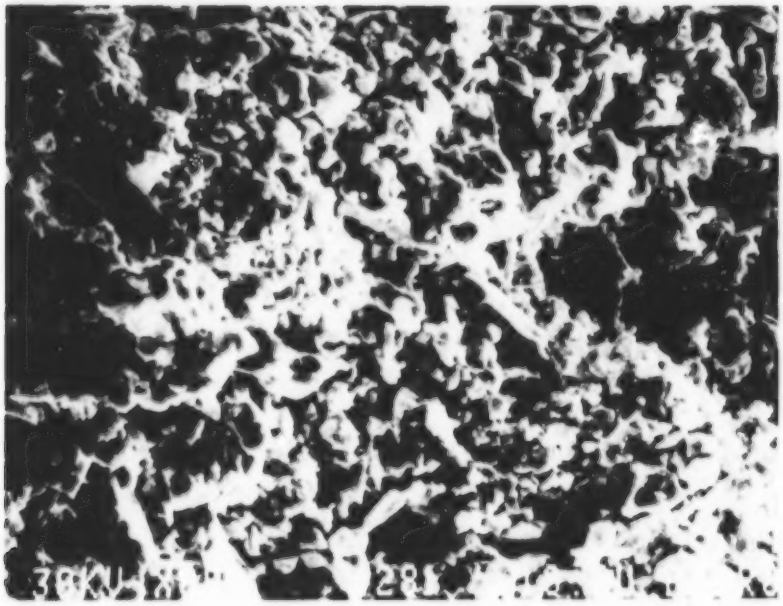

FIGURE 8

SCANNING ELECTRON MICROGRAPH OF COLD-PRESSED AND FRACTURED $YBa_2Cu_3O_{7-x}$ SPECIMEN (DENSITY 4.32 g/cm^3).

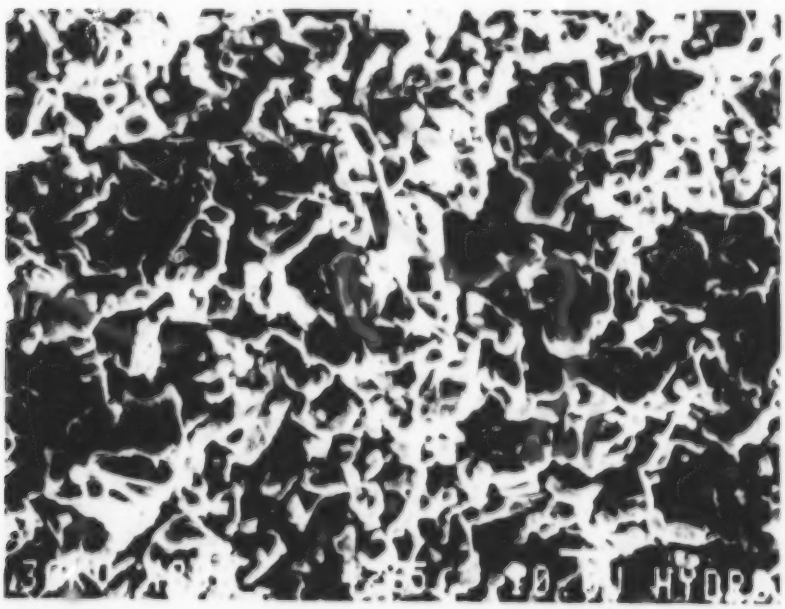

FIGURE 9

SCANNING ELECTRON MICROGRAPH OF SINTERED AND FRACTURED $YBa_2Cu_3O_{7-x}$ SPECIMEN AT 945°C FOR 18 HOURS (DENSITY 4.42 g/cm^3).

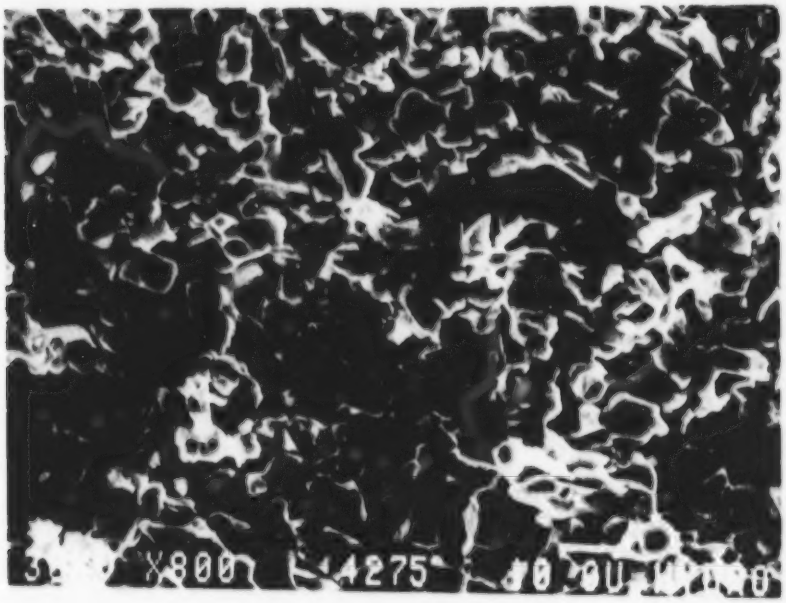

FIGURE 10

SCANNING ELECTRON MICROGRAPH OF SINTERED AND FRACTURED $YBa_2Cu_3O_{7-x}$ SPECIMEN AT 965°C FOR 18 HOURS (DENSITY 5.06 g/cm^3).

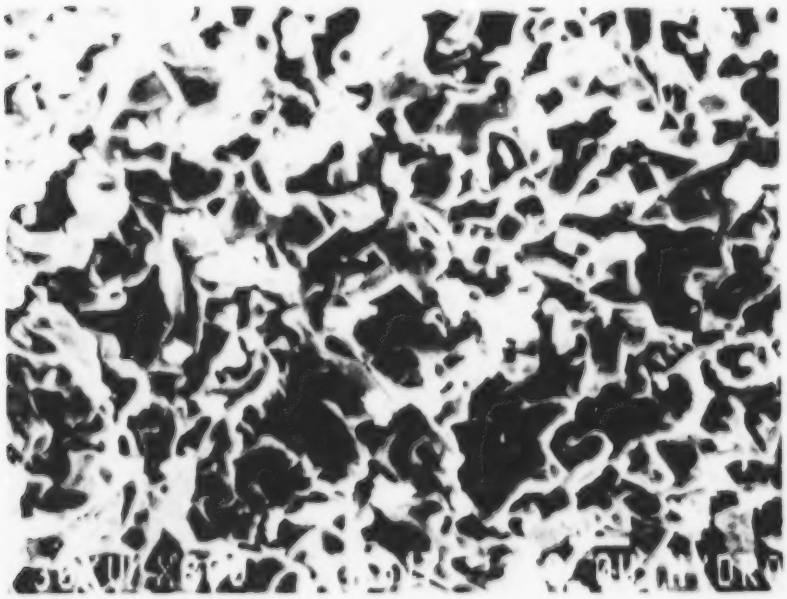

FIGURE 11

SCANNING ELECTRON MICROGRAPH OF SINTERED AND FRACTURED $YBa_2Cu_3O_{7-x}$ SPECIMEN AT 985°C FOR 18 HOURS (DENSITY 5.24 g/m^3).

178546-K8-RD

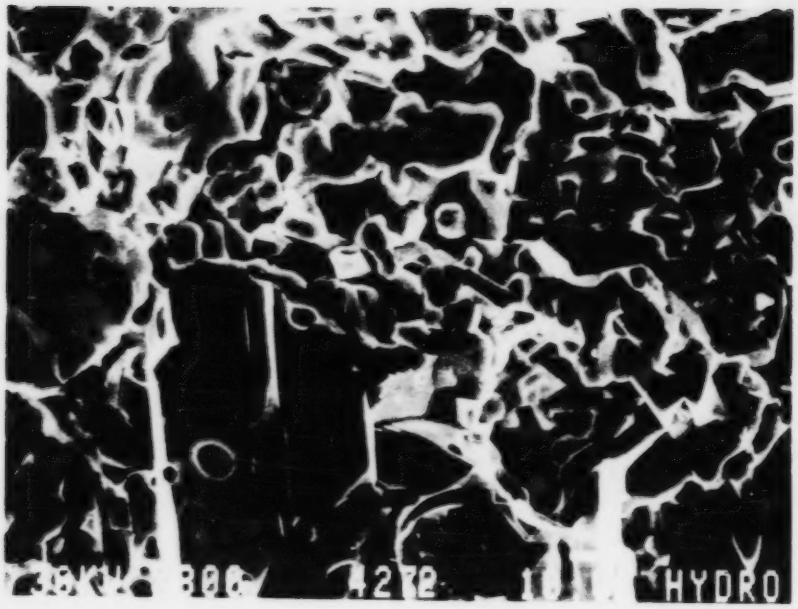

FIGURE 12

SCANNING ELECTRON MICROGRAPH OF SINTERED AND FRACTURED $YBa_2Cu_3O_{7-x}$ SPECIMEN AT 985°C FOR 67 HOURS (DENSITY 5.39 g/cm^3).

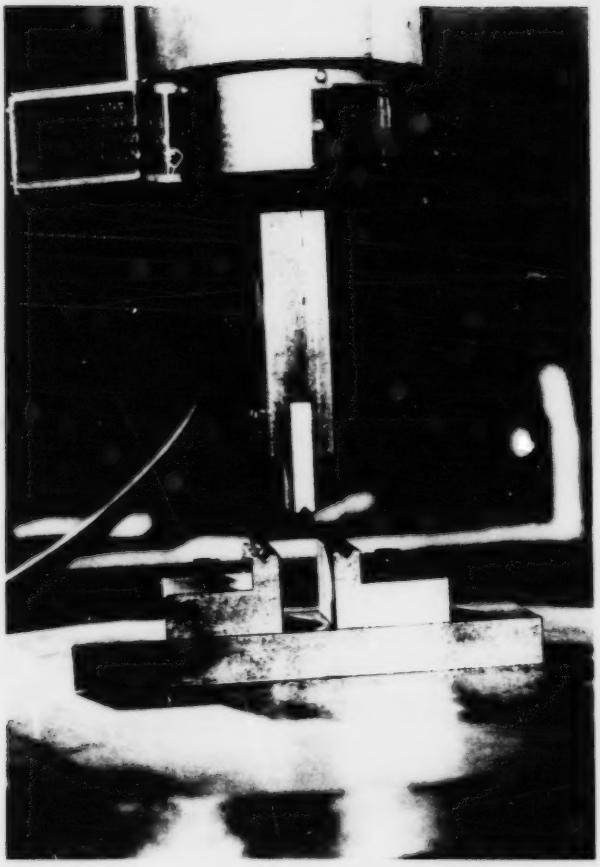

FIGURE 13

VIEW OF THE TREE POINT BEND TEST LOADING ASSEMBLY.

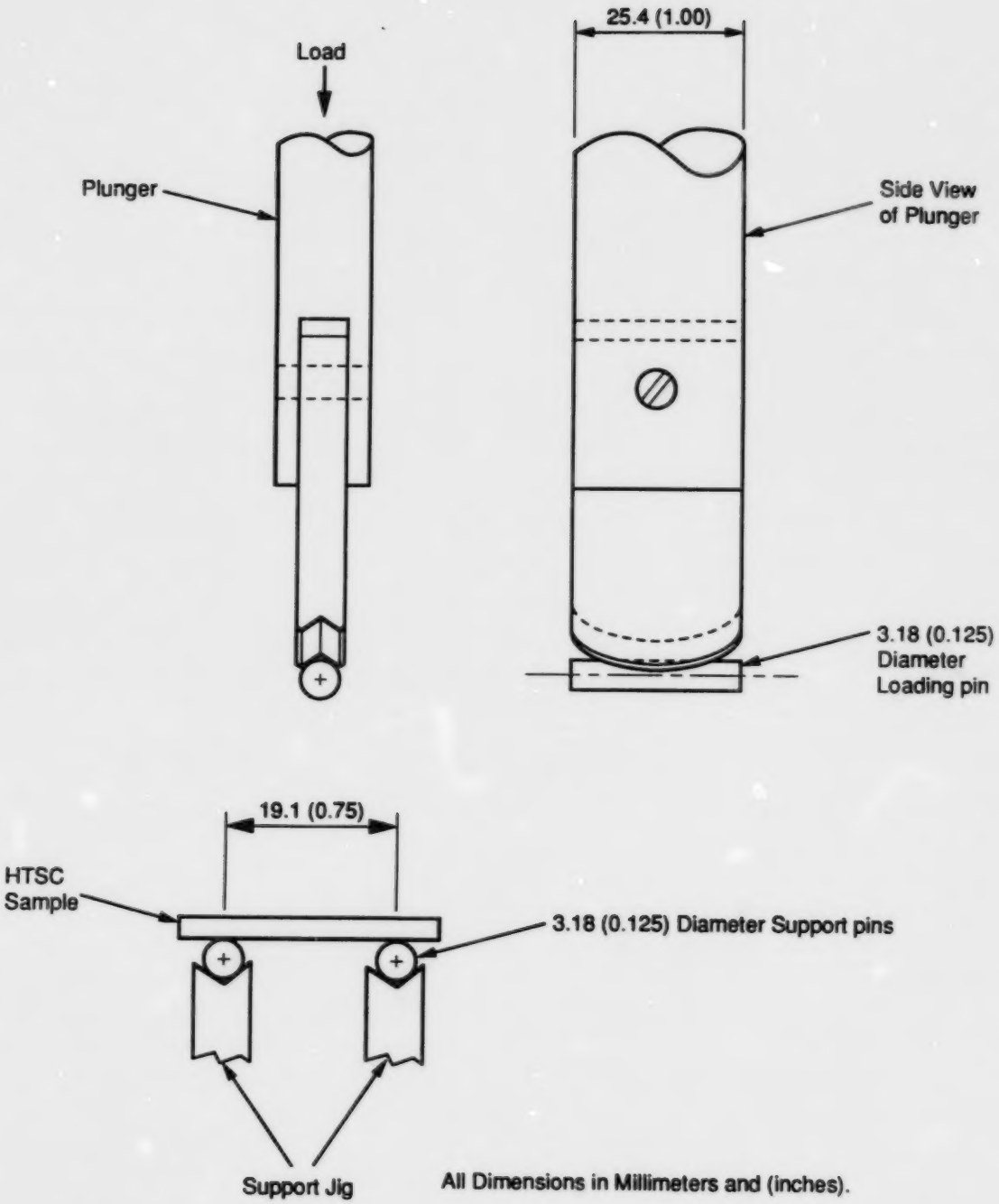

FIGURE 14

SCHEMATIC OF THE SAMPLE LOADING ARRANGEMENT.

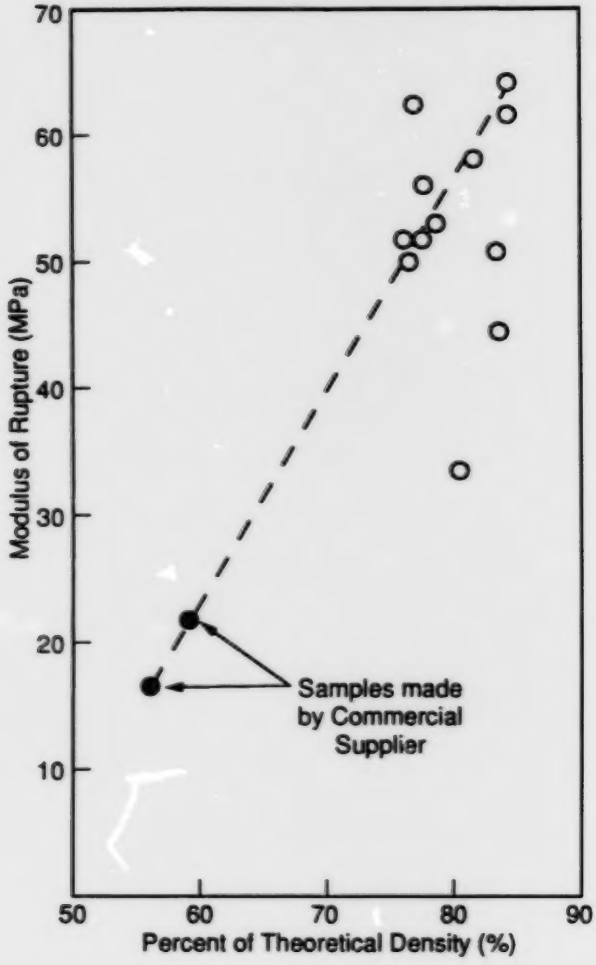

FIGURE 15

RELATIONSHIP BETWEEN MODULUS OF RUPTURE AND DENSITY OF THE $YBa_2Cu_3O_{7-x}$ MATERIAL.

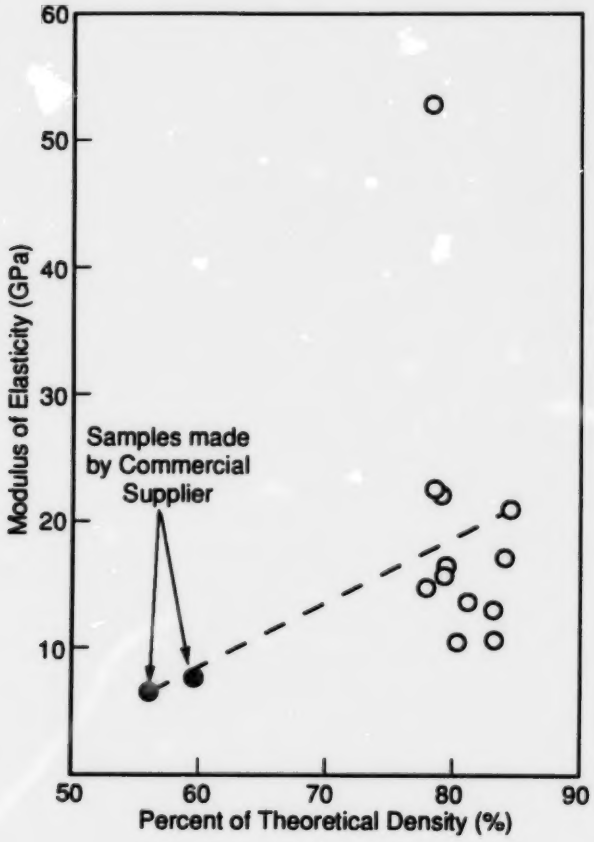

FIGURE 16

RELATIONSHIP BETWEEN MODULUS OF ELASTICITY AND DENSITY OF $YBa_2Cu_3O_{7-X}$ MATERIAL.

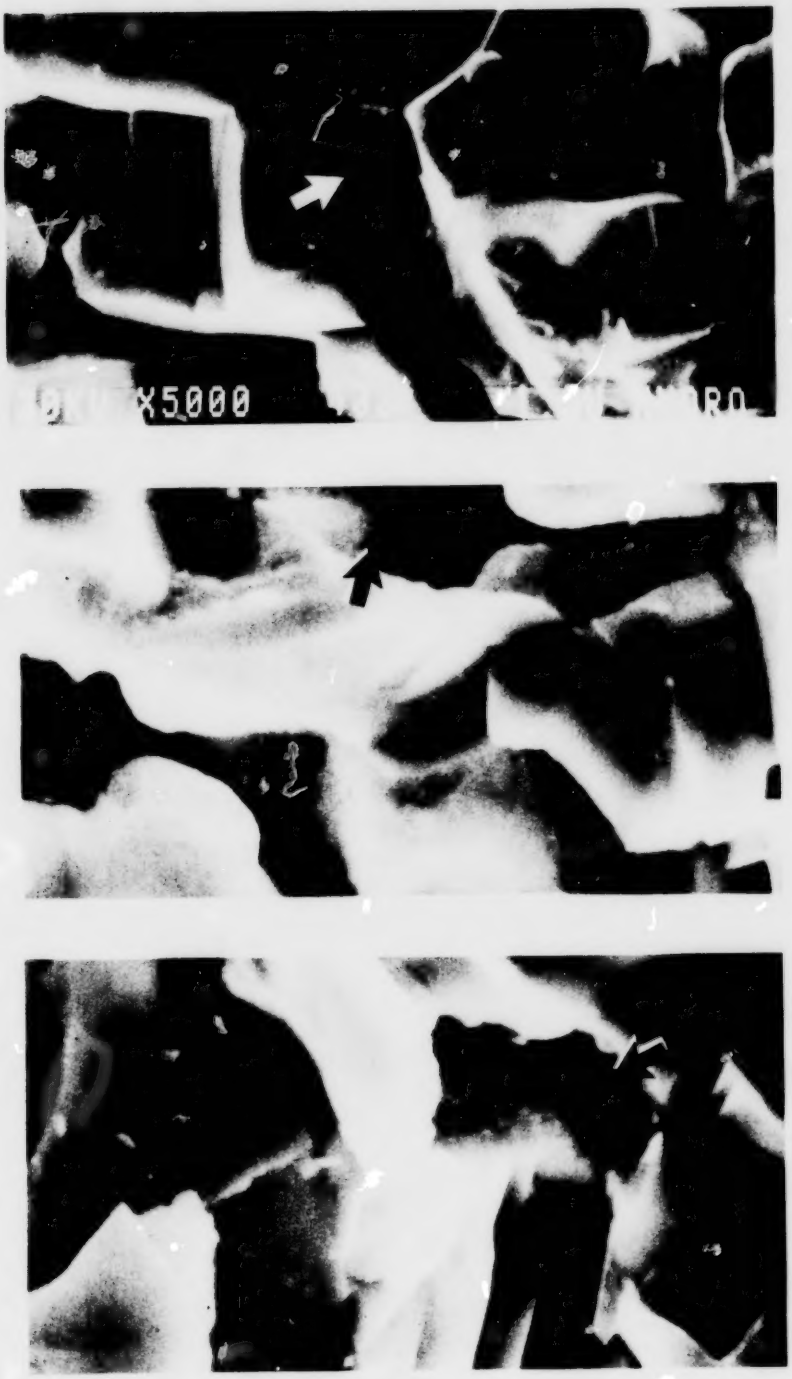

FIGURE 17

FRACTURE SURFACES OF $YBa_2Cu_3O_{7-x}$ (OHRD MADE) AFTER THERMAL CYCLING (50°C→BOILING LIQUID NITROGEN→50°C, AND MECHANICAL TESTING. THE ARROWS POINT TO INTERCONNECTED CHANNELS OF PORES.

182353-K8-RD

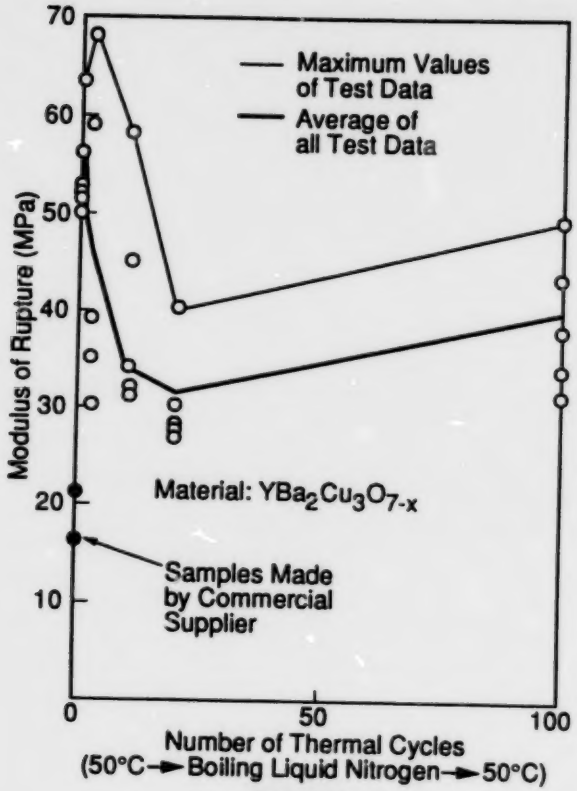

FIGURE 18

EFFECT OF THERMAL CYCLING ON MODULUS OF RUPTURE.

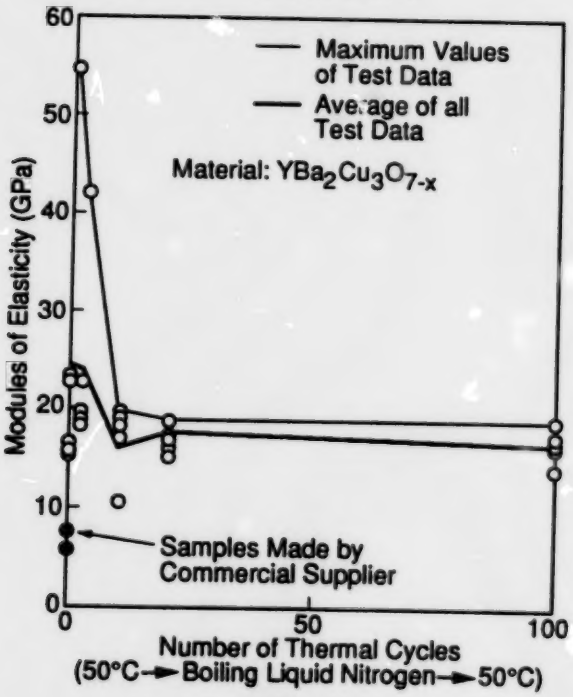

FIGURE 19

EFFECT OF THERMAL CYCLING ON MODULUS OF ELASTICITY.

182366-A23-RD

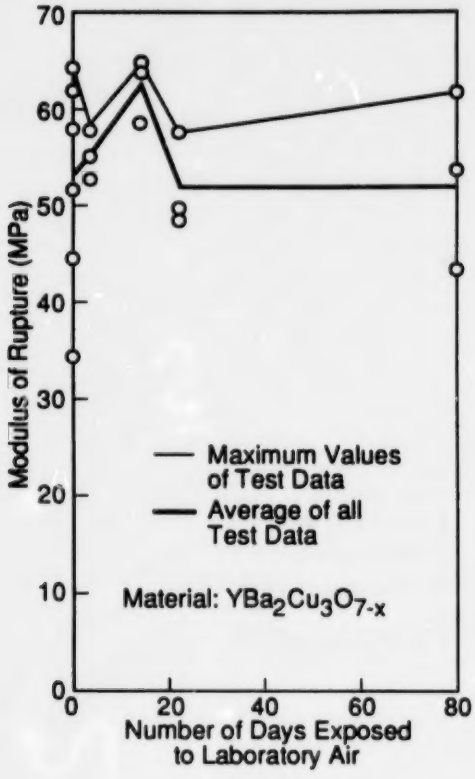

FIGURE 20

EFFECT OF EXPOSURE TO LABORATORY AIR ON MODULUS OF RUPTURE.

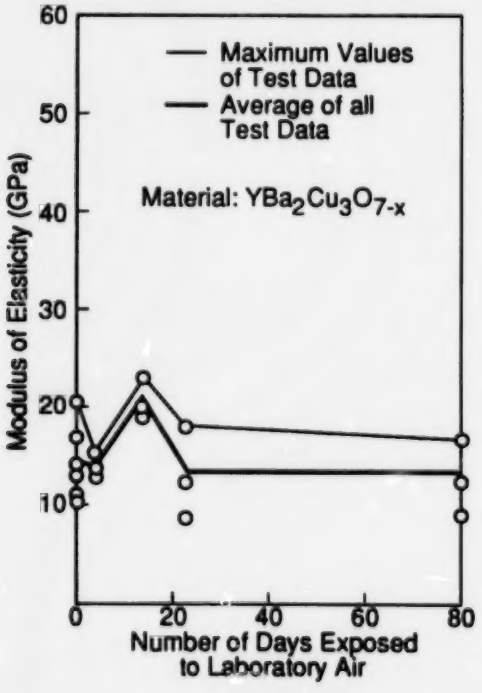

FIGURE 21

EFFECT OF EXPOSURE TO LABORATORY AIR ON MODULUS OF RUPTURE.

182367-A23-RD

TABLE I

Nominal Composition of Y-Ba-Cu-O Materials
Prepared in this Program

Sample Number and Identification		Chemical Formula Y_A-Ba_B-Cu_C-O_{7-x}		
		A	B	C
1	(1-2-3)	1	2	3
2	(0-2-3)	0	2	3
3	(0.5-2-3)	0.5	2	3
4	(1.5-2-3)	1.5	2	3
5	(1-0-3)	1	0	3
6	(1-1.5-3)	1	1.5	3
7	(1-1-3)	1	1	3
8	(1-2.5-3)	1	2.5	3
9	(1-2-0)	1	2	0
10	(1-2-2.5)	1	2	2.5
11	(1-2-1)	1	2	1
12	(1-2-3.5)	1	2	3.5

TABLE II
Effect of Temperature and Time on
Density of Sintered Specimens

Sample Number and Identification (Y-Ba-Cu)	Sintering Conditions		Density	
	Temperature (°C)	Time (hrs)	g/cm^3	% of Theoretical
(1-2-3)			6.38*	100
(1-2-3)	not sintered cold pressed only (207 MPa)		4.32	67.7
1 (1-2-3)	945	18	4.42	69.3
1A (1-2-3)	965	18	5.06	79.3
1B (1-2-3)	985	18	5.24	82.1
1C (1-2-3)	985	67	5.39	84.5
2 (0-2-3)	945	18	did not sinter	
3 (0.5-2-3)	945	18	4.54	-
4 (1.5-2-3)	945	18	4.20	-
5 (1-0-3)	945	18	did not sinter	
6 (1-1.5-3)	945	18	4.71	-
7 (1-1-3)	945	18	4.87	-
8 (1-2.5-3)	945	18	3.68	-
9 (1-2-0)	945	18	did not sinter	
10 (1-2-2.5)	945	18	3.93	-
11 (1-2-1)	945	18	did not sinter	
12 (1-2-3.5)	945	18	8.67	-

* Theoretical density calculated from chemical formula $YBa_2Cu_3O_{7-x}$ and unit cell volume.

TABLE III

Results of EDX Analysis of Sintered
$YBa_2Cu_3O_{7-x}$ Material

	Composition		
Analysed Element	Nominal* (at %)	Relative** X-Ray Intensity (%)	ZAF*** Corrected (at %)
Yttrium	16.7	38.1	16.6
Barium	33.3	42.1	33.1
Copper	50	19.8	50.3

* Nominal (at %): As compounded before calcining and sintering

** Relative X-ray Intensity (%): As measured x-ray intensity for a given element divided by sum of x-ray intensities of all three elements (Y, Ba, Cu) and multiplied by 100.

*** ZAF Corrected (at %): Corrected for atomic number, absorption and fluorescence effects. Procedure is embedded in data processing program of the instrument.

TABLE IV

Nominal and Analyzed Composition o Y-Ba-Cu
Using Energy Dispersive X-Ray Spectrometry (EDX)

Sample Number and Identification	Composition								
	Yttrium			Barium			Copper		
	Nominal* (at %)	Relative** X-Ray Intensity (%)	ZAF Corrected (at %)	Nominal (at %)	Relative X-Ray Intensity (%)	ZAF Corrected (at %)	Nominal (at %)	Relative X-Ray Intensity (%)	ZAF Corrected (at %)
1 (1-2-3)	16.7	38.1	16.6	33.3	42.1	33.2	50	19.8	50.2
2 (0-2-3)									
3 (0.5-2-3)									
4 (1 5-2-3.0)	23.1	46.5	21.1	30.8	35.23	29.6	46.1	18.5	49.3
5 (1-0-3)									
6 (1-1.5-3)									
7 (1-1-3)	20.0	62.2	30.3	20.0	20.3	18.2	60.0	17.5	51.5
8 (1-2.5-3)									
9 (1-2-0)									
10 (1-2-2.5)									
11 (1-2-1)									
12 (1-2-3.5)	15.4	37.8	16.0	30.8	40.5	30.5	53.8	21.7	53.5

* Nominal (at %): As compounded before calcining and sintering.

** Relative X-Ray Intensity (%): As measured X-Ray intensity for a given element divided by a sum of X- Ray Intensity of all three (Y, Ba, Cu) elements and multiplied by 100.

*** ZAF Corrected (at %): Corrected for atomic number, absorption and fluorescence effects. Correction procedure is embedded in data processing program of the analyzer.

TABLE V

Results of Tests To Determine The Effect of Thermal Cycling
($50^{o}C$-Boiling Liquid Nitrogen-$50^{o}C$) on Mechanical Properties of $YBa_2Cu_3O_{7-x}$ Material

Sample No.	Thermal Cycles (No.)	Sample Dimensions			Weight (g)	Volume (cm^3)	Density (g/cm^3)	% of Theoretical Density	Load at Failure (N)	Sample Deflection at Failure (mm)	Modulus of Rupture (MPa)	At Midpoint of Elastic Range		Modulus of Elasticity (MPa)
		Width (mm)	Thickness (mm)	Length (mm)								Load (N)	Sample Deflection (mm)	
1	As Made at OHRD	6.12	3.48	24.13	2.545	0.514	4.95	77.6	163.46	0.040	63.02	81.65	0.02	54767
2	"	6.15	3.38	24.23	2.488	0.503	4.95	77.6	128.4	0.051	52.22	64.2	0.021	22792
3	"	6.15	3.32	24.2	2.466	0.495	4.98	78.1	123.97	0.049	52.25	61.98	0.022	22141
4	"	6.12	3.30	24.18	2.442	0.489	4.99	78.3	132.86	0.067	56.96	66.43	0.033	15583
5	"	6.10	3.32	24.16	2.478	4.90	5.06	79.3	125.08	0.06	53.16	62.54	0.030	16131
6	"	6.15	3.23	24.28	2.385	4.81	4.95	77.6	113.96	0.06	50.75	56.98	0.030	15221
1	Made by Commercial Supplier	6.40	3.12	24.94	1.794	4.99	3.59	56.4	36.12	0.047	16.57	18.6	0.024	6833
2	"	6.40	3.10	25.63	1.914	5.08	3.76	59.0	47.24	0.057	21.95	23.62	0.029	7513
1	2	6.10	3.35	24.1	2.503	0.493	5.08	79.6	85.05	0.035	35.50	45.53	0.018	18313
2	2	6.12	3.35	24.1	2.501	0.495	5.06	79.2	163.46	0.030	68.0	81.73	0.015	40929
3	2	6.10	3.35	24.1	2.475	0.493	5.02	78.7	73.39	0.030	30.63	36.7	0.015	18436
4	2	6.05	3.23	23.95	2.384	0.467	5.10	80.0	86.74	0.035	39.27	43.37	0.019	21009
5	2	6.10	3.30	24.08	2.478	0.485	5.11	80.1	137.31	0.059	59.10	68.7	0.03	18349

TABLE V - CONTINUED

Results of Tests To Determine The Effect of Thermal Cycling
($50^{o}C$-Boiling Liquid Nitrogen-$50^{o}C$) on Mechanical Properties of $YBa_2Cu_3O_{7-x}$ Material

Sample No.	Thermal Cycles (No.)	Sample Dimensions			Weight (g)	Volume (cm^3)	Density (g/cm^3)	% of Theoretical Density	Load at Failure (N)	Sample Deflection at Failure (mm)	Modulus of Rupture (MPa)	At Midpoint of Elastic Range		Modulus of Elasticity (MPa)
		Width (mm)	Thickness (mm)	Length (mm)								Load (N)	Sample Deflection (mm)	
1	10	6.10	3.33	24.1	2.491	0.489	5.09	79.9	65.03	0.030	27.47	32.52	0.015	16632
2	10	6.07	3.33	24.05	2.476	0.486	5.10	79.9	67.83	0.030	28.80	33.92	0.015	17434
3	10	6.10	3.33	24.05	2.503	0.488	5.13	80.4	62.81	0.030	26.53	31.4	0.015	16065
4	10	6.07	3.43	24.03	2.554	0.500	5.11	80.03	90.61	0.06	36.26	45.31	0.03	10656
5	10	6.07	3.33	24.13	2.501	0.487	5.13	80.43	116.76	0.05	49.57	58.38	0.025	18006
1	20	6.05	3.25	24.1	2.406	0.474	5.08	79.6	61.16	0.030	27.35	30.58	0.015	16965
2	20	6.10	3.25	24.13	2.436	0.478	5.09	79.8	67.83	0.030	30.08	33.92	0.015	18661
3	20	6.10	3.28	24.05	2.472	0.480	5.15	80.6	92.83	0.050	40.42	46.42	0.025	14907
4	20	6.07	3.43	24.03	2.558	0.500	5.11	80.2	72.28	0.030	28.92	36.14	0.015	16916
5	20	6.07	3.43	24.05	2.562	0.500	5.12	80.2	67.83	0.030	27.14	33.92	0.015	16953
1	100	6.07	3.45	24.08	2.589	0.505	5.12	80.3	97.86	0.040	38.70	48.93	0.020	16964
2	100	6.10	3.38	24.13	2.575	0.497	5.18	81.2	75.62	0.041	31.00	37.81	0.021	13533
3	100	6.07	3.38	24.05	2.564	0.493	5.20	81.5	104.5	0.043	43.06	52.25	0.022	17920
4	100	6.07	3.38	24.10	2.520	0.494	5.19	81.3	119.0	0.053	49.04	59.5	0.027	16556
5	100	6.07	3.45	24.03	2.559	0.504	5.08	79.6	88.39	0.037	34.96	44.20	0.019	16565

TABLE VI

Results of Tests To Determine The Effect of Exposure to Laboratory Air to Laboratory Air on Mechanical Properties of $YBa_2Cu_3O_{7-x}$ Material

Sample No.	Exposure Days	Sample Dimensions			Weight (g)	Volume (cm^3)	Density (g/cm^3)	% of Theoretical Density	Load at Failure (N)	Sample Deflection at Failure (mm)	Modulus of Rupture (MPa)	At Midpoint of Elastic Range		Modulus of Elasticity (MPa)
		Width (mm)	Thickness (mm)	Length (mm)								Load (N)	Sample Deflection (mm)	
1	As Made at OHRD	5.96	3.32	23.55	2.512	0.468	5.37	84.2	149.02	0.067	64.81	74.51	0.034	17625
2	"	5.96	3.48	23.57	2.612	0.489	5.34	83.7	130.11	0.067	51.51	63.06	0.034	13362
3	"	5.94	3.38	23.55	2.529	0.473	5.34	83.7	106.76	0.069	44.95	53.38	0.035	11659
4	"	5.89	3.40	23.47	2.532	0.470	5.38	84.3	148.13	0.053	62.17	74.07	0.027	20866
5	"	6.02	3.34	23.58	2.470	0.474	5.211	81.6	136.78	0.071	58.20	68.39	0.036	14844
6	"	6.06	3.42	23.80	2.521	0.493	5.113	80.1	84.52	0.057	34.07	42.26	0.029	10572
1	3.5	5.94	3.43	23.60	2.569	0.481	5.34	83.7	141.23	0.067	57.75	70.62	0.034	15199
2	3.5	5.99	3.43	23.65	2.540	0.486	5.22	81.8	135.67	0.071	55.01	67.84	0.036	13663
3	3.5	5.92	3.43	23.57	2.582	0.478	5.40	84.6	126.77	0.069	52.01	63.39	0.035	13292
1	14	5.94	3.28	23.52	2.473	0.458	5.40	84.6	131.22	0.057	58.67	65.61	0.029	18982
2	14	5.97	3.43	23.50	2.567	0.481	5.34	83.6	157.91	0.049	64.24	78.96	0.025	23120
3	14	5.92	3.30	23.57	2.495	0.461	5.41	84.8	145.90	0.057	64.67	72.95	0.029	20794
1	22	6.04	3.44	23.52	2.541	0.489	5.196	81.4	120.10	0.096	48.01	60.05	0.048	8794
2	22	6.00	3.38	23.62	2.512	0.479	5.244	82.2	139.01	0.057	57.95	69.51	0.029	18193
3	22	6.04	3.32	23.44	2.416	0.470	5.140	80.6	115.65	0.075	49.64	57.83	0.038	12058
1	80	6.00	3.46	23.58	2.564	0.489	5.24	82.1	153.46	0.063	61.05	76.73	0.032	16939
2	80	6.08	3.58	23.64	2.680	0.514	5.21	81.6	145.01	0.071	53.18	72.51	0.036	12654
3	80	5.98	3.44	23.60	2.526	0.485	5.21	81.6	107.20	0.079	43.29	53.6	0.040	9634